

Analysis of Microtubule Dynamics Using Growth Curve Models

S. Rao Jammalamadaka*

University of California Santa Barbara

Md. Aleemuddin Siddiqi*

Symbiance, Inc.

Kaushik Ghosh

University of Nevada Las Vegas

June 16, 2008

Abstract

Microtubules are part of the structural network within a cell's cytoplasm, providing structural support as well as taking part in many of the cellular processes. A large body of data provide evidence that dynamics of microtubules in a cell is responsible for the performance of many critical cellular functions such as cell division. In this article, we study the effect of four different isoforms of a protein tau on microtubule dynamics using growth curve models. The results show that a linear growth curve model is sufficient to explain the data. Moreover, we find that a mutated version of 3-repeat tau protein has a similar effect as a 4-repeat tau protein on microtubule dynamics. The latter findings conform with the biological understanding of the effect of the protein tau on microtubule dynamics.

1 Introduction

Microtubules are sub-cellular structures present in most plant and animal cells and form what is known as the cytoskeleton (see Alberts et al., 2002,

*This work is supported by the National Science Foundation Grant # 0331697.

Avila, 1990). They are cytoplasmic fibers with a tubular form, composed of several strands linked by lateral interactions. A combination of biochemical, structural and morphological analyses during the past three decades have shown that the cytoplasm of a cell is not a disorganized mass of jelly but a highly structured cell compartment formed of a cytoskeleton, one of whose principal components are microtubules.

Studies have revealed that microtubules are not only well organized but are highly dynamic (see Mitchison and Kirschner, 1984, Jordan and Wilson, 2004). By dynamic, we mean that they undergo changes in length over time. A microtubule which grows and/or shortens very rapidly is said to be highly dynamic. The dynamics of the microtubules are induced by their polymerization and depolymerization. This, in turn, affects all the microtubule induced-cellular functions such as cell shape, intracellular transport, chromosome segregation and flagella mediated cell motility (see Feinstein and Wilson, 2005).

The dynamics of microtubules in living cells has been of great importance in studying certain diseases and their treatments. For instance, promising anti-cancer drugs suppress cell division by stabilizing microtubule activity. It is thus of interest to study the dynamics of these microtubules under different treatments and conditions.

In this article, we study the effect of various isoforms of a protein called tau on microtubule dynamics using statistical growth curve analysis. Using rigorous statistical analyses and tests, we are able to confirm or refute various biological hypotheses about the microtubules under differing treatment conditions. We observe in our analysis that a mutated 4-Repeat tau i.e., where G272 has been mutated to V has a similar effect on microtubule dynamics as the 3-Repeat tau. This supports the structure function model of the biochemical interaction of the tau protein on the microtubules.

2 Microtubule Dynamics

Microtubule images in living cells are acquired by fluorescence microscopy. The images are in the form of a video which is essentially a stack of still-images taken over successive time intervals. Figure 1 gives one such still-image of various microtubules. In each stack, a certain number of microtubules are selected and tracked, i.e. their individual coordinate locations are noted for each image in the stack by the experimenter.



Figure 1: Microtubule tips are tracked manually or automatically. Picture courtesy Professors Stuart Feinstein, Leslie Wilson and Dr. Janis Bunker of the Department of Molecular Cellular and Developmental Biology, UCSB.

By observing a stack/video of the microtubules, the experimenter chooses some microtubules whose tips are easy to track. These microtubule tips are then tracked in each frame. For each microtubule, one fixes the initial position $\mathbf{p}_0 = (a_0, b_0)$ (i.e. where the microtubule is attached and seems to grow out of) as the initial observation or the origin. Then for each succeeding frame i , the tip's pixel location $\mathbf{p}_i = (a_i, b_i)$ is noted. The Euclidean distance between the points \mathbf{p}_0 and \mathbf{p}_i i.e., $\| \mathbf{p}_i - \mathbf{p}_0 \|$ represents the approximate length of the microtubule in frame number i .

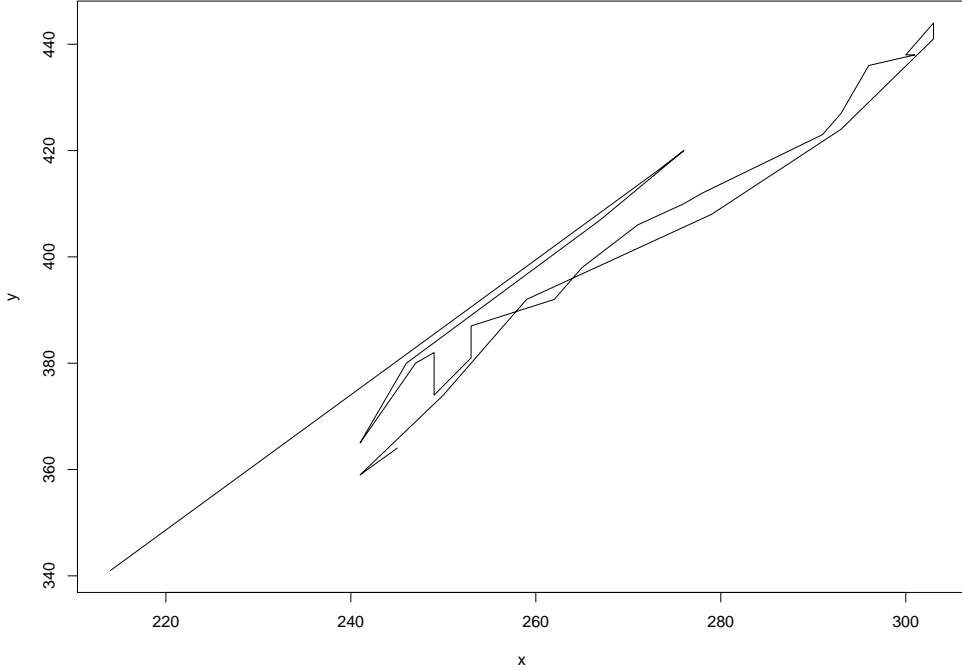


Figure 2: The path traversed by a typical microtubule tip. The first point(origin) is the location of one end of the microtubule. Data courtesy Professors Stuart Feinstein, Leslie Wilson and Dr. Janis Bunker of the Department of Molecular Cellular and Developmental Biology, UCSB.

Figure 2 gives an example of the path taken by the sequence $\mathbf{p}_0, \mathbf{p}_1, \mathbf{p}_2, \dots$ in a typical microtubule. In practice, not all microtubules can be tracked for the same number of frames, as some microtubules are lost or become denatured before others. Hence, for each tip, the tracking sequence can be of different length. As a preliminary analysis, for our illustrative example, we consider only those microtubules which could be tracked for the full set of frames (the number of which is denoted by n). For each microtubule, we compute the length sequence $\{l_i\}$ given by,

$$l_i = \{(a_i - a_0)^2 + (b_i - b_0)^2\}^{\frac{1}{2}}; \quad i = 1, 2, \dots, n. \quad (1)$$

For most in-vivo microtubules, the tip locations, $\mathbf{p}_1, \mathbf{p}_2, \dots$ are reasonably along a straight line, as can be seen in Figure 2. In view of this, we define our “growth variable” $x(i)$, $i = 1, 2, \dots, n$ as the cumulative change in length up till frame i . Hence,

$$x(i) = \sum_{j=1}^i |l_j - l_{j-1}|, \quad (2)$$

where we take $l_0 = l_1$, making $x(1) = 0$. This growth variable is our measure of the dynamics of each microtubule and will be used for our growth curve analyses in this paper. Our growth curve for a particular microtubule is thus defined by $x(i)$, $i = 1, 2, 3, \dots, n$.

Note that an alternative measure of dynamics is given by

$$y(i) = \sum_{j=1}^i \|\mathbf{p}_j - \mathbf{p}_{j-1}\|.$$

Such a measure would perhaps be more appropriate when the path is not as linear as in Figure 2 and is hence not used in this research.

3 Growth Curve Modeling

Suppose that there are r different treatments (or groups) and x is the real-valued growth variable measured at p different time points: t_1, t_2, \dots, t_p for n_j individuals chosen at random from the j^{th} treatment. Such correlated data over time, labeled “Growth curves,” can be analyzed using the methods introduced in Potthoff and Roy (1964). It has been discussed and analyzed later by several authors, significant among them being Khatri (1966), Grizzle and Allen (1969), Rao (1973), Pan and Fang (2001) and Sengupta and Jammalamadaka (2003). Using specialized packages, one can also do exact tests for growth curve models, details of which can be found in Weerahandi (2004).

We consider the following polynomial regression model of degree $(q - 1)$ for the mean growth of x for the j^{th} treatment on the time variable t ,

$$E(x_j(t)) = \psi_{j0}t^0 + \psi_{j1}t^1 + \dots + \psi_{j,q-1}t^{q-1} \quad (3)$$

for $t = t_1, \dots, t_p$; $j = 1, \dots, r$ with $p > q - 1$. Let

$$\boldsymbol{\psi}'_j = (\psi_{j0} \ \psi_{j1} \ \dots \ \psi_{jq-1}) \quad (4)$$

denote the vector of the growth curve coefficients for the j^{th} treatment. The observations $x_j(t_1), \dots, x_j(t_p)$, being on the same specimen, are correlated, and we denote their variance-covariance matrix by $\boldsymbol{\Sigma}$. We assume $\boldsymbol{\Sigma}$ to be the same for all the r groups. Assuming n_j observations in the j^{th} group, let \mathbf{X}_j denote the $p \times n_j$ matrix of the observations for the j^{th} group. Since our growth variable sequence obtained for each of the microtubules starts with $x_1 = 0$, this first value is redundant. It will make the design matrix \mathbf{X} (Equation 5) singular and is thus omitted. Let

$$\mathbf{X} = [\mathbf{X}_1 \mathbf{X}_2 \dots \mathbf{X}_r]. \quad (5)$$

\mathbf{X} is a $p \times N$ matrix of all the observations where

$$N = n_1 + n_2 + \dots + n_r. \quad (6)$$

Therefore from Equation (3) we get,

$$\begin{aligned} E(\mathbf{X}_j) &= [\mathbf{B}\boldsymbol{\psi}_j \mathbf{B}\boldsymbol{\psi}_j \dots \mathbf{B}\boldsymbol{\psi}_j] \\ &= \mathbf{B}\boldsymbol{\psi}_j \mathbf{E}_{1n_j} \quad (j = 1, 2, \dots, r), \end{aligned} \quad (7)$$

where

$$\mathbf{B} = \begin{bmatrix} t_1^0 & t_1^1 & \dots & t_1^{q-1} \\ t_2^0 & t_2^1 & \dots & t_2^{q-1} \\ \dots & \dots & \dots & \dots \\ t_p^0 & t_p^1 & \dots & t_p^{q-1} \end{bmatrix} \quad (8)$$

and \mathbf{E}_{ab} denotes, a matrix of order $a \times b$ with all elements equal to 1. $\mathbf{B}_{p \times q}$ is called the ‘‘Design Matrix’’. From Equation (7), we get

$$\begin{aligned} E(\mathbf{X}) &= [\mathbf{B}\boldsymbol{\psi}_1 \mathbf{E}_{1n_1} | \mathbf{B}\boldsymbol{\psi}_2 \mathbf{E}_{1n_2} | \dots | \mathbf{B}\boldsymbol{\psi}_r \mathbf{E}_{1n_r}] \\ &= \mathbf{B}\boldsymbol{\psi} \mathbf{A}, \end{aligned} \quad (9)$$

where

$$\boldsymbol{\psi} = [\boldsymbol{\psi}_1 \dots \boldsymbol{\psi}_r] \tag{10}$$

is the $q \times r$ matrix of the growth curve coefficients and

$$\mathbf{A} = \text{diag}[\mathbf{E}_{1n_1}, \mathbf{E}_{1n_2}, \dots, \mathbf{E}_{1n_r}], \tag{11}$$

is a block diagonal matrix with \mathbf{E}_{1n_j} ($j = 1, 2, \dots, r$) along the diagonal blocks and zeros elsewhere. \mathbf{A} is of order $r \times N$.

Let $\text{Vec}\mathbf{X}$ be defined as the column vector obtained by stacking the columns of \mathbf{X} one below the other. Denoting $\text{Var}(\text{Vec}\mathbf{X})$ by $\text{Var}(\mathbf{X})$, we find that

$$\text{Var}(\mathbf{X}) = \mathbf{I}_N \otimes \boldsymbol{\Sigma}, \tag{12}$$

where \otimes denotes the Kronecker product of two matrices. Equations (9) and (12) define what is called the Growth Curve Model and considerable detail on this topic can be found in Kshirsagar and Smith (1995), Pan and Fang (2001).

4 Data Description

Tau is a protein which plays a major role in microtubule dynamics and stability. Biologists have a biochemical structural model for the mechanisms by which the various isoforms of tau attach to the microtubules and affect their dynamics. Under these models, the 4-repeat (4R) units of tau are the main units by which it attaches to the microtubule (Figure 3). Similarly 3-repeat (3R) units of tau play the main role in attachment to the microtubule. 3R tau is the dominant tau isoform found in human fetuses while 4R tau appears mostly in adults. 4RGV is a mutant of 4R in the second repeat unit i.e. G272 has been mutated to V (denoted by G272V). This mutation is known to cause fronto-temporal dementia with Parkinsonism-like symptoms (FTDP-17) in humans and to affect the ability of 4R-tau to regulate microtubule dynamics. Under the biochemical models, 4RGV is expected to behave like 3R tau in binding to the microtubules. If true, the microtubules treated with 3R should have similar dynamics as those treated with 4RGV.

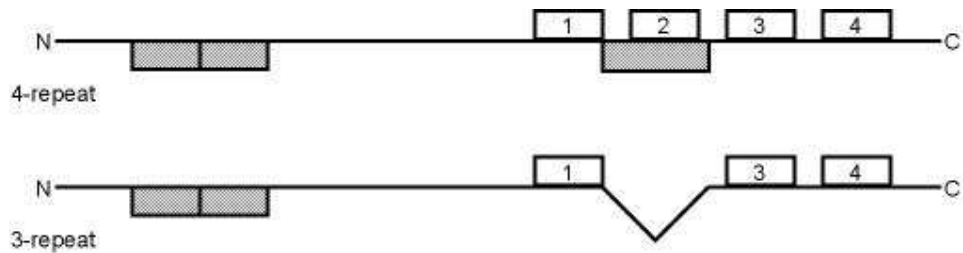


Figure 3: 4R and 3R tau schematic.

Data on microtubules were collected by Professors Stuart Feinstein, Leslie Wilson and Dr. Janis Bunker of the Department of Molecular Cellular and Developmental Biology, UCSB. In this paper we analyze the microtubule dynamics for 4 different classes — the control (or un-injected untreated microtubules), and 3 treatments, which we describe briefly. In our modest study, we have 4 treatment groups (including the Control) as follows:

1. **Control:** These are for the normal cells with no treatments. There are 27 observations in this class.
2. **3R:** These are for cells injected with 3-repeat (3R) tau. There are 22 observations in this class.
3. **4R:** These are for cells injected with 4-repeat (4R) tau. There are 20 observations in this class.
4. **4RGV:** These are for cells injected with the G272V mutant of 4R tau. There are 16 observations in this class.

Hence, there was a total of $N=85$ observations in all the categories combined. Figure 4 shows the plots for the growth variable x for these different treatment groups.

5 Growth Curve Analysis

To fit the growth curve model and to test various hypotheses, we perform the following computations, which are described more fully in Kshirsagar

and Smith (1995). For our analysis, we chose Σ to have the Rao's simple covariance structure:

$$\Sigma = \mathbf{B}\Gamma\mathbf{B}' + \mathbf{Q}\Theta\mathbf{Q}'$$

where Γ is a $q \times q$ positive definite matrix, Θ is a $(p - q) \times (p - q)$ positive definite matrix and \mathbf{Q} is a $p \times (p - q)$ matrix of rank $p - q$ with $\mathbf{B}'\mathbf{Q} = \mathbf{0}$. This ensures that the maximum likelihood estimates and the generalized least squares estimates coincide. Other general structures of the covariance matrix Σ are possible, but were not used, since they require iteratively reweighted least squares procedures, which need large amounts of data. Under this assumption, the maximum likelihood estimator of the coefficient matrix ψ is given by (see Pan and Fang, 2001)

$$\hat{\psi} = (\mathbf{B}'\mathbf{S}^{-1}\mathbf{B})^{-1}(\mathbf{B}'\mathbf{S}^{-1}\mathbf{X})\mathbf{A}'(\mathbf{A}\mathbf{A}')^{-1} \quad (13)$$

where

$$\mathbf{S} = \mathbf{X}[\mathbf{I} - \mathbf{A}'(\mathbf{A}\mathbf{A}')^{-1}\mathbf{A}]\mathbf{X}'.$$

5.1 Model Selection

The first step would be to determine the degree $q - 1$ of the polynomial in the growth curve model that adequately fits the data. To do this, we test the hypothesis

$$H_0^* : \text{the degree } (q - 1) \text{ of the growth curves is adequate.} \quad (14)$$

To do this, we first obtain a matrix \mathbf{B}_2 of order $p \times (p - q)$ such that

$$\mathbf{B}_2'\mathbf{B} = \mathbf{0}, \quad (15)$$

where \mathbf{B} is as in Equation (8). This can be done by choosing $(p - q)$ linearly independent columns of $[\mathbf{I}_p - \mathbf{B}(\mathbf{B}'\mathbf{B})^{-1}\mathbf{B}']$.

Next we compute,

$$\mathbf{S} = \mathbf{X}(\mathbf{I} - \mathbf{A}'(\mathbf{A}\mathbf{A}')^{-1}\mathbf{A})\mathbf{X}', \quad (16)$$

where \mathbf{A} is defined in (11).

For each hypothesis testing problem, we need the following degrees of freedom (d.f.),

$$\begin{aligned} d_m &= \text{order of the error or hypothesis matrix,} \\ d_E &= \text{d.f. associated with the error matrix,} \\ \text{and } d_H &= \text{d.f. associated with the hypothesis matrix.} \end{aligned}$$

For this purpose, we construct the MANOVA table given in Table 1.

Source	d.f.	Dispersion, order $(p - q = 22)$
H_0^*	$r = 4$	$\mathbf{H}_0 = \mathbf{B}'_2 \mathbf{X} [\mathbf{A}' (\mathbf{A} (\mathbf{A} \mathbf{A}')^{-1} \mathbf{A}) \mathbf{X}' \mathbf{B}_2$
Error	$N - r = 81$	$\mathbf{E}_0 = \mathbf{B}'_2 \mathbf{S} \mathbf{B}_2$
Total	$N = 85$	$\mathbf{H}_0 + \mathbf{E}_0 = \mathbf{B}'_2 \mathbf{X} \mathbf{X}' \mathbf{B}_2$

Table 1: MANOVA for testing Model Adequacy

We construct the matrix of observations $\mathbf{X}_{24 \times 85}$ and obtain the design matrix $\mathbf{B}_{24 \times q}$ from Equation (8). To perform the test we construct the Wilks' Λ statistic defined by,

$$\Lambda_0 = \frac{|\mathbf{E}_0|}{|\mathbf{E}_0 + \mathbf{H}_0|}. \quad (17)$$

To test the null hypothesis we use the fact (see eg. Rao, 1973, Sec. 8c.5) that the null distribution of

$$F = \frac{1 - \Lambda_0^{\frac{1}{s}}}{\Lambda_0^{\frac{1}{s}}} \times \frac{ms - 2\lambda}{d_H d_m} \quad (18)$$

is approximately an F_{ν_1, ν_2} where,

$$\begin{aligned} \nu_1 &= d_m d_H \\ \nu_2 &= ms - 2\lambda \end{aligned}$$

and

$$\begin{aligned} m &= N - \frac{d_m + d_H + 1}{2} \\ s &= \left(\frac{(d_m d_H)^2 - 4}{d_m^2 + d_H^2 - 5} \right)^{\frac{1}{2}} \\ \lambda &= (d_m d_H - 2)/4. \end{aligned}$$

q	Λ_0	F	p -value
1	0.0291	3.7062	4.4409E-16
2	0.3228	0.9018	0.7099

Table 2: Summary of model adequacy tests for various growth curve models. $q - 1$ is the degree of polynomial, Λ_0 is the Wilks' Lambda statistic and F is the corresponding F approximation.

In our case, $p = 24$ and $N = n_1 + n_2 + n_3 + n_4 = 27 + 22 + 20 + 16 = 85$.

The results of the tests for $q = 1$ and $q = 2$ are summarized in Table 2.

Based on the results, we see that a constant model (no change in time) is rejected but a linear fit for the growth-curve provides an adequate fit, and the model is well specified. Under the model that the mean growth function is linear, we show the plots for the mean curves in Figure 5. Figure 5 also shows how these linear fitted means for each class compare with the (non-parametric) observed means, computed as the mean at each time point for all the functions in that class. Figure 6 gives the error band (formed from the maximum and minimum observed value at each timepoint) and the fitted curve for the control group. Based on the picture, the model fits the observed data quite well.

Remark: Most curve-fitting techniques such as the polynomials, do not provide for local control of shape. Consequently, local change (for example change in the observed function at one time point) in a polynomial fit affects the entire fitted curve. The B -spline curve avoids this problem by using a special set of blending functions that has only local influence and depends on only a few neighboring control points.

The *spline regression* model for x on the time variable t is given by

$$E(x_j(t)) = \psi_{j0}s_0(t) + \psi_{j1}s_1(t) + \cdots + \psi_{jq-1}s_{q-1}(t), \quad (19)$$

for $t = t_1, t_2, \dots, t_p$; $p > q - 1$; $j = 1, 2, \dots, r$. Here $s_0(\cdot), \dots, s_{q-1}(\cdot)$ are the basis functions. Then, the growth-curve coefficients for the j^{th} treatment becomes

$$\psi'_j = (\psi_{j0} \ \psi_{j1} \ \dots \ \psi_{jq-1}). \quad (20)$$

See, for example, James and Hastie (2001), Mortenson (1985) for further details. Such B-splines can also be used to fit the data. Most of the analysis, as well as the testing is very similar to what has been described so far, except that the Design Matrix \mathbf{B} given in (8) is to be replaced by

$$\mathbf{B} = \begin{bmatrix} s_0(t_1) & s_1(t_1) & \dots & s_{q-1}(t_1) \\ s_0(t_2) & s_1(t_2) & \dots & s_{q-1}(t_2) \\ \dots & \dots & \dots & \dots \\ s_0(t_p) & s_1(t_p) & \dots & s_{q-1}(t_p) \end{bmatrix}. \quad (21)$$

Such spline bases are likely to be useful when dealing with non-steady-state data. For the steady-state data that we have dealt with in this analysis, linear fits seem to do perfectly fine as expected.

5.2 Comparison of Treatments

Next we test if the 4 groups, namely the control and the 3 treatments are significantly different. Hence we test the hypothesis

$$\begin{aligned} H_1^* &: \boldsymbol{\psi}_1 = \boldsymbol{\psi}_2 = \dots = \boldsymbol{\psi}_4 \\ &: \mathbf{L}\boldsymbol{\psi}\mathbf{M} = 0; \end{aligned} \quad (22)$$

where,

$$\mathbf{L} = \mathbf{I}_2 \text{ and } \mathbf{M} = \begin{bmatrix} 1 & 0 & 0 \\ 0 & 1 & 0 \\ 0 & 0 & 1 \\ -1 & -1 & -1 \end{bmatrix}.$$

To test this hypothesis we construct the MANOVA table given in Table 3:

Source	d.f.	Dispersion, order ($p - q = 22$)
H_1^*	$m = 3$	$\mathbf{H}_1 = (\mathbf{L}\hat{\boldsymbol{\psi}}\mathbf{M})(\mathbf{M}'\mathbf{R}_{11}\mathbf{M})^{-1}(\mathbf{L}\hat{\boldsymbol{\psi}}\mathbf{M})'$
Error	$N - r - (p - q) = 59$	$\mathbf{E}_1 = \mathbf{L}(\mathbf{B}'\mathbf{S}^{-1}\mathbf{B})^{-1}\mathbf{L}'$
Total	$N - r - (p - q) + m = 62$	$\mathbf{H}_1 + \mathbf{E}_1$

Table 3: MANOVA table for Testing H_1^*

where \mathbf{R}_{11} in Table 3 is defined by,

$$\mathbf{R}_{11} = (\mathbf{A}\mathbf{A}')^{-1}[\mathbf{I} + \mathbf{A}\mathbf{X}' \times \{ \mathbf{S}^{-1}\mathbf{B}(\mathbf{B}\mathbf{S}^{-1}\mathbf{B})^{-1} \} \mathbf{X}\mathbf{A}'(\mathbf{A}\mathbf{A}')^{-1}]. \quad (23)$$

Based on Table 2, we calculate the following Wilks' Λ statistic,

$$\Lambda_1 = \frac{|\mathbf{E}_1|}{|\mathbf{E}_1 + \mathbf{H}_1|} = 0.5564. \quad (24)$$

and the corresponding F-statistic (with $d_m = 2$) to be

$$F_1 = \frac{1 - \sqrt{\Lambda_1}}{\sqrt{\Lambda_1}} \cdot \frac{(d_E - 1)}{d_H} = 6.5851. \quad (25)$$

Under the hypothesis H_1^* , F_1 has an F distribution with $df = (2d_H, 2d_E - 2) = (6, 116)$. The p -value of this test thus turns out to be approximately = 0.0. Hence H_1^* is rejected, indicating at least one of the growth curves significantly differ from the rest.

Next, we perform pairwise comparisons to see how the classes compare to one another. These were carried out by fitting the model to two classes at a time and testing the appropriate linear hypotheses for the equality of the polynomial coefficients (taken to be linear here). Table 4 summarizes these results.

Pair	Wilks' Λ	p -value
*3R vs control	0.6839	0.0185
*4R vs control	0.4112	1.3836E-4
*4RGV vs control	0.4842	0.0043
3R vs 4R	0.8655	0.3150
3R vs 4RGV	0.9004	0.5616
4R vs 4RGV	0.8399	0.4179

Table 4: p -values of various pairwise comparisons. * denotes a significant pair.

These p -values show that there is significant difference between the following pairs: 3R vs control, 4R vs control and 4RGV vs control. It is worth noting that the p -value for the pair (3R, 4RGV) is the highest, indicating that they are quite similar in their dynamics – confirming the widely believed bio-chemical structure function model of the biologists.

6 Conclusion

We have provided a novel statistical analysis of the dynamics of microtubules. Our analysis supports the widely held beliefs of biochemical functioning of microtubules and their responses to various treatments.

7 Acknowledgements

The authors would like to thank Professors Stuart Feinstein and Leslie Wilson as well as Dr. Janis Bunker of the Department of Molecular Cellular and Developmental Biology, UCSB for helping us with the biological interpretations and for providing the original data sets. They also wish to express thanks to Professor B.S. Manjunath of the Electrical and Computer Engineering department at UCSB for the opportunity to collaborate on this bioinformatics project.

The authors would also like to thank two anonymous referees for their detailed comments which led to several improvements in the presentation.

References

- Alberts, B., Johnson, A., Lewis, J., Raff, M., Roberts, K., and Walters, P. (2002), *Molecular Biology of the Cell*, London: Garland Science.
- Avila, J. (1990), “Microtubule Dynamics,” *FASEB Journal*, 4, 3284–3290.
- Feinstein, S. C. and Wilson, L. (2005), “Inability of Tau to Properly Regulate Neuronal Microtubule Dynamics: A Loss-of-function Mechanism by which Tau might Mediate Neuronal Cell Death,” *Biochimica et Biophysica Acta*, 1739, 268–279.
- Grizzle, J. E. and Allen, D. M. (1969), “Analysis of Growth and Dose Response Curves,” *Biometrics*, 25, 357–381.
- James, G. and Hastie, T. (2001), “Functional Linear Discriminant Analysis for Irregularly Sampled Curves,” *Journal of the Royal Statistical Society, Series B*, 63, 533–550.
- Jordan, M. A. and Wilson, L. (2004), “Microtubules as Target for Anticancer Drugs,” *Nature Reviews Cancer*, 4, 253–265.

- Khatri, C. G. (1966), "A Note on MANOVA Model Applied to Problems in Growth Curves," *Annals of the Institute of Statistical Mathematics*, 18, 75–86.
- Kshirsagar, A. M. and Smith, W. B. (1995), *Growth Curves*, New York: Marcel Dekker.
- Mitchison, T. and Kirschner, M. (1984), "Dynamic Instability of Microtubule Growth," *Nature*, 312, 237–242.
- Mortenson, M. E. (1985), *Geometric Modeling*, New York: John Wiley & Sons.
- Pan, J.-X. and Fang, K.-T. (2001), *Growth Curve Models and Statistical Diagnostics*, New York: Springer-Verlag.
- Potthoff, R. and Roy, S. N. (1964), "A Generalized Multivariate Analysis of Variance Model Useful Especially for Growth Curve Problems," *Biometrika*, 51, 313–326.
- Rao, C. R. (1973), *Linear Statistical Inference*, New York: John Wiley & Sons, 2nd ed.
- Sengupta, D. and Jammalamadaka, S. R. (2003), *Linear Models – An Integrated Approach*, Singapore: World Scientific.
- Weerahandi, S. (2004), *Generalized Inference in Repeated Measures*, New York: John Wiley & Sons.

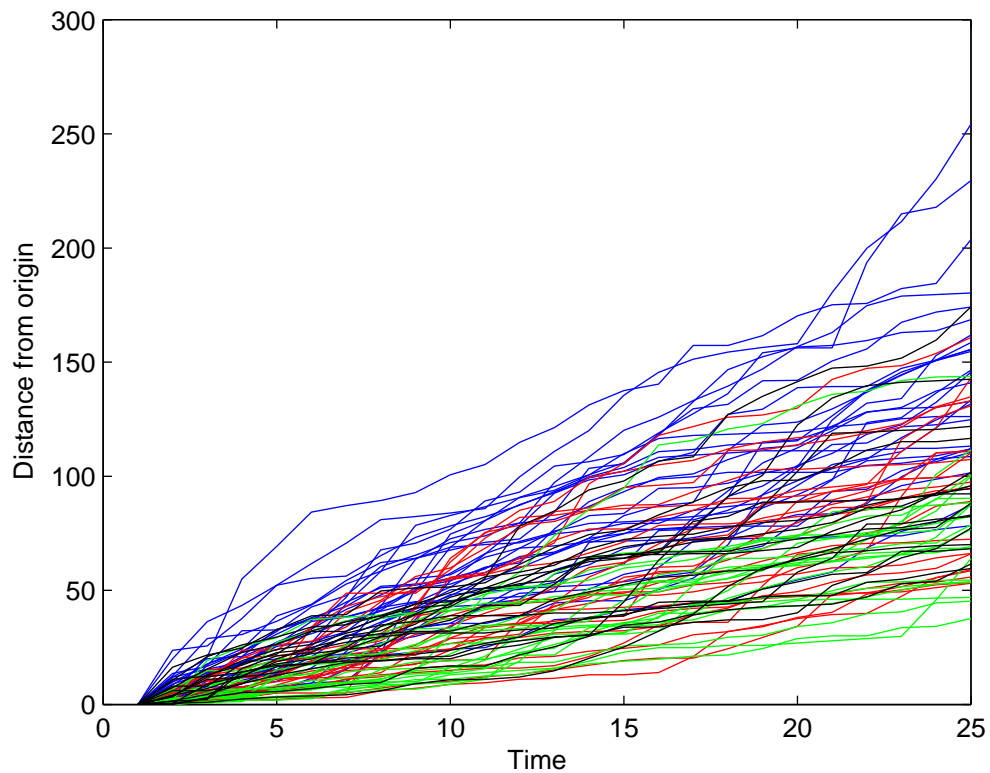


Figure 4: Growth variables for the different treatment groups. **Blue**: Control, **Red**: 3R, **Green**: 4R, **Black**: 4RGV. Data courtesy Professors Stuart Feinstein, Leslie Wilson and Dr. Janis Bunker of the Department of Molecular Cellular and Developmental Biology, UCSB.

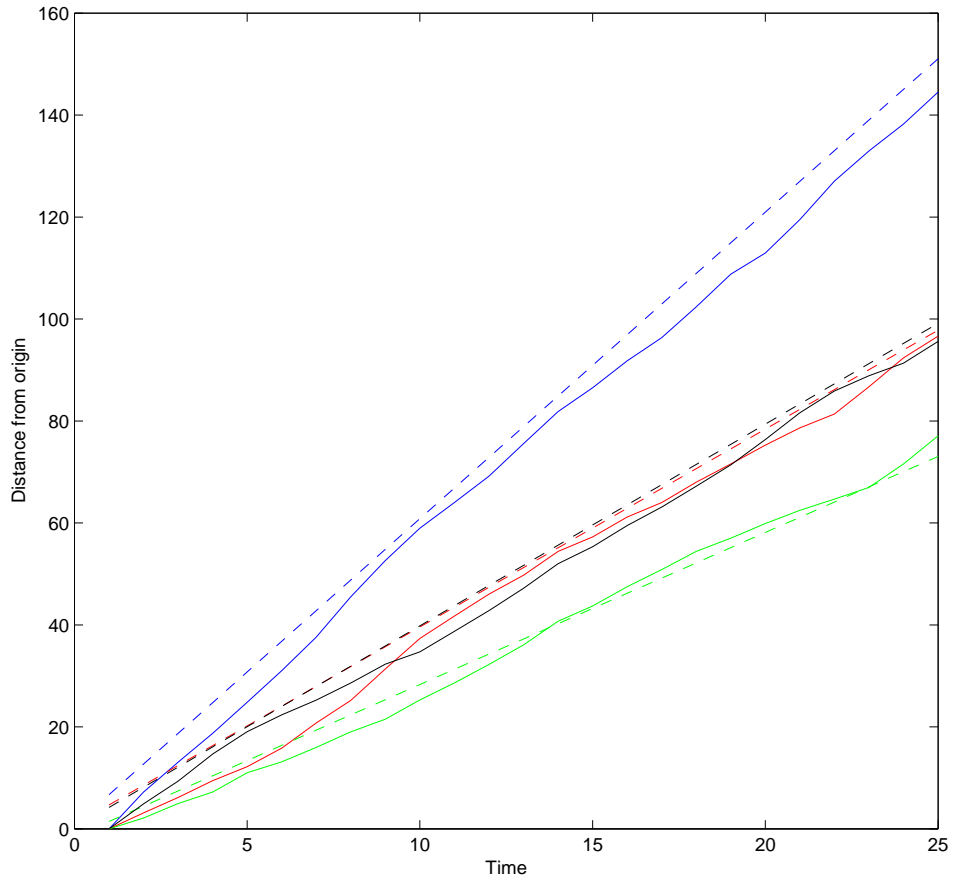


Figure 5: The observed means (solid lines) and the fitted means (dotted lines) using a linear (first order polynomial) growth curve.

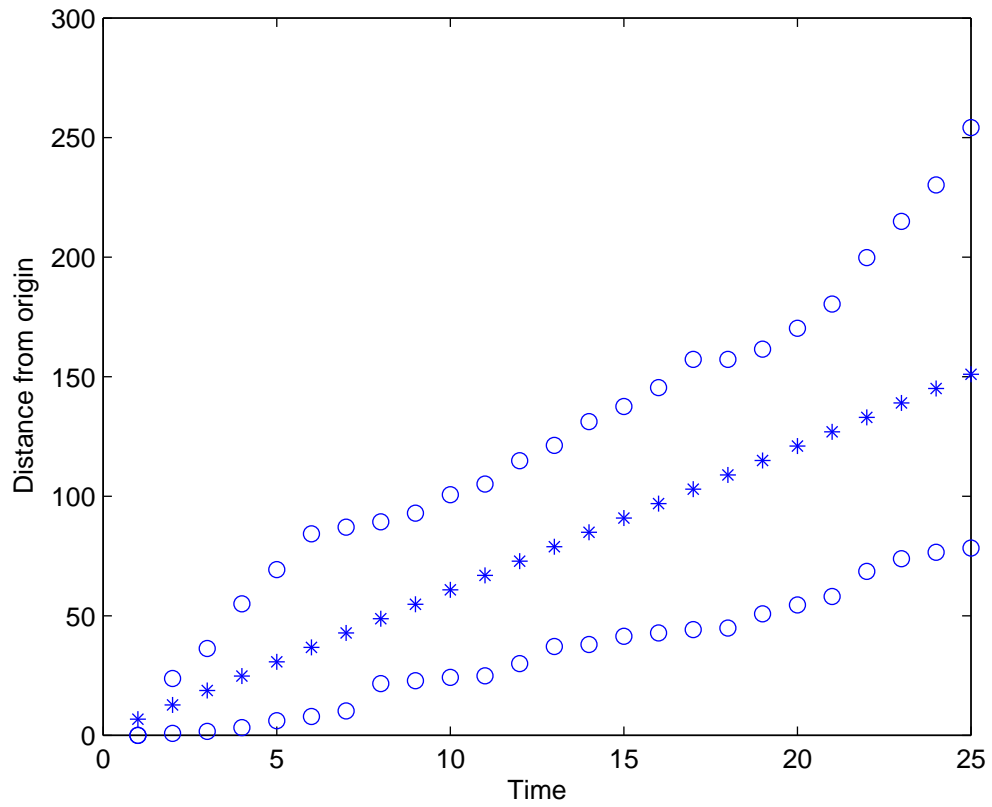


Figure 6: The error band from the observed data (o) and linear fit (*) for the control group.